VYSOKÉ UČENÍ TECHNICKÉ V BRNĚ
BRNO UNIVERSITY OF TECHNOLOGY

FAKULTA CHEMICKÁ
ÚSTAV CHEMIE MATERIÁLŮ

FACULTY OF CHEMISTRY
INSTITUTE OF MATERIALS SCIENCE

THE CRYSTALLIZATION KINETICS IN SEMICRYSTALLINE NANOCOMPOSITES

KINETIKA KRYSTALIZACE V SEMIKRYSTALICKÝCH NANOKOMPOZITECH

DIZERTAČNÍ PRÁCE
DOCTORAL THESIS

AUTOR PRÁCE
AUTHOR
Ing. KATEŘINA HYNŠTOVÁ

VEDOUCÍ PRÁCE
SUPERVISOR
prof. RNDr. JOSEF JANČÁŘ,CSc.

BRNO 2010

ABSTRACT

The crystal growth greatly affects morphology and, thus, physical properties of semicrystalline polymers. In this PhD work, the effect of adding high specific surface area silica nano-filler on the crystallization kinetics of linear polyethylene was investigated. In polymers, adding high specific surface area filler is able to alter the chain dynamics even at very low filler loadings. It is suggested that in the vicinity of the filler surface, polymer chains exhibit retarded reptation motion due to the chain immobilization caused by either the filler-polymer interaction or by chain constraints between closely packed nanoparticles.

The polarized optical microscope equipped with a hot stage was employed to measure the spherulites growth rates in the medium crystallization regime II. It was shown that even weak interaction between PE chains and silica nano-filler above glass transition temperature leads to substantial decrease of the spherulite growth rate. The measured data were correlated with predictions based on the theoretical models and molecular simulations of molecular dynamics of the crystallizing polymer.

The observed decrease of spherulite growth rate, G, in dependence on both the silica nano-filler content and polyethylene molecular weight was interpreted utilizing the chain immobilization hypothesis, where the dynamics adsorption and desorption of the chain at the filler interface results in the slowing down of the reptation motion.

Keywords: polyethylene, nanocomposite, crystallization kinetics, reduced reptation

ABSTRAKT

Růst krystalů zásadně ovlivňuje morfologii a tím také fyzikální vlastnosti semikrystalických polymerů. Tato PhD práce přináší alternativní pohled na popis kinetiky krystalizace v polyolefinech plněných slabě interagujícími částicemi. V nanokompozitních materiálech vysoký specifický povrch plniva i při nízkých plněních zásadně ovlivňuje dynamiku řetězců. V blízkosti povrchu plniva začíná hrát významnou roli zpomalená reptace způsobená jak vzájemnými interakcemi plnivo-polymer tak prostorovým omezením mezi nanočásticemi.

Růst krystalů byl zkoumán pomocí polarizovaného optického mikroskopu vybaveného horkým stolkem. Výsledky byly korelovány s teoretickými modely a rozsáhlými počítačovými simulacemi na molekulární úrovni.

Pozorovaný pokles rychlosti růstu sférolitů v závislosti na obsahu plniva a molekulové hmotnosti matrice je interpretován na základě imobilizační hypotézy.

Klíčová slova: Polyetylen, nanokompozit, kinetika krystalizace, zpomalená reptace

TABLE OF CONTENTS

POLYMER CRYSTALLIZATION

Many useful materials in the future are expected to be created with various self-organizing molecules. Crystallization is a typical case of polymer self-organization, which has long been investigated since the discovery of chain-folding as the principal mode of crystallization. The chain-folded lamellae are main building blocks of polymeric materials and their spatial distribution dominates all physicochemical properties of the materials. Crystal structures and crystallization mechanisms are therefore central subjects in science and technology of polymers.

Also in most processing technologies, crystallization process can affect physical properties of final articles made of semicrystalline polymers, substantially. The kinetics of polymer crystallization is controlled by the diffusion of chains to the phase transition zone. Changes in morphology brought about by a change in temperature or by the external factors will cause changes in physical properties and in the response to an applied stress. Thus, due to the close relation between the properties and morphology, the nature and consequences of the changes connected with the nanoparticles addition must be fully understood.

The nature of the polymer nanocomposites research is shifting the main emphasis on the research of fundamental aspects of physics of long chain molecules in both non-Newtonian liquids and disordered and ordered solids. New phenomena now observed on the micro-scale are being discovered with huge potential application benefits. Despite its importance, no generally acceptable explanation of the peculiarities of the development of the crystalline structure observed in nanocomposites with semicrystalline matrices has been published in the scientific literature so far.

Crystallization of flexible polymers with a large number of internal degrees of freedom involves very complicated molecular motions of various space and time scales, ranging from large scale transport of whole chains to atomistic scale rearrangement of crystalline stems in perfecting crystalline order. In contrast to the global chain dynamics in the melt, the molecular motions during crystallization can be very sensitive to the chemical structure just like the crystal structure being specific to the structure of constituent molecules.

Many stereo-regular polymers, whether synthetic or biological, form partially crystalline solids, which consist of crystalline lamellae and intervening amorphous layers [1]. The crystalline polymers are known to show characteristic multi-scale structures ranging from local crystalline structure to macroscopic structure of spherulites (Fig. 1). Since the morphology is closely related to the properties, it is in the focus of the scientific interest continuously [2-4]. The crystal structure of polymer is almost uniquely determined as the lowest free-energy state, and the energy analyses by computer modeling have contributed much to the structure determinations [5-7]. On the other hand, the large-scale structure, the way of lamellar stacking or branching for example, may be determined by the balance of equilibrium and kinetic processes of crystallization. They show a great deal of varieties depending on the crystallization conditions such as temperature, pressure, solvent as well as on molecular structure itself [1, 8-10].

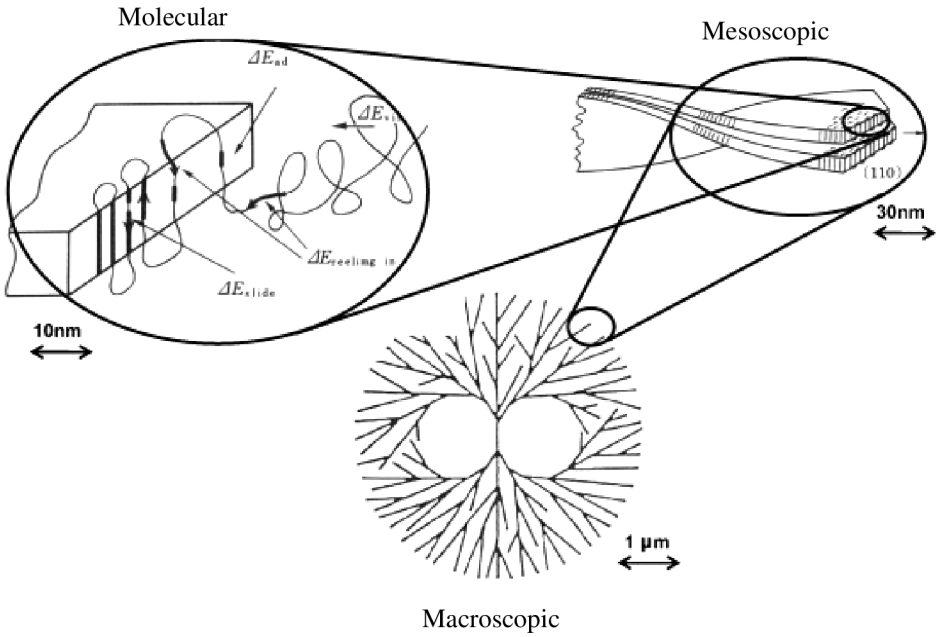

Figure 1: Multi-scale structures of crystalline polymers, from molecular-level structure of the lamella crystal growing by reeling in random coiled chains in the melt, to mesoscopic level structure of growing lamellae showing cooperative layering and twisting, and to final macroscopic spherulitic aggregate of the lamella [11].

On the basis of the secondary nucleation mechanism, a framework of the molecular scenario was first proposed by Lauritzen and Hoffman (LH) soon after the discovery of chain-folded crystallization [12-15]. Due to the great success of the LH-theory especially in predicting characteristic changes in lamellar thickness and crystal growth rate with crystallization temperature T_c, most of the discussions thereafter have been concentrated on understanding various experiments in terms of the LH-theory.

As for the very beginning of crystallization in isotropic melt, the presence of unknown impurities in polymer samples has long obscured the primary nucleation mechanism. Recent surge of investigations on the very early stages of crystallization will have an origin in the proposal of peculiar instability in undercooled melt before the onset of crystallization, a spinodal-decomposition (SD) or phase-separation assisted nucleation scenario [16].

Emerging also is the new enthusiasm about novel crystallization in strongly confined systems; very thin film [17] polymers in a cylindrical cavities or nanorods [18] or nanodomains in phase separated block-copolymers [19] and [20].The presence of surface or interface will cause strong constraints on polymer conformations and enforce peculiar chain trajectories during crystallization.

The polymer crystallization thus involves quite new topics as well as historical unsolved problems. Long flexible polymers are considered to show chain-folded crystallization from highly entangled states by reeling in their chain tails. The experimental knowledge available is mostly macroscopic, and detailed molecular processes of polymer

crystallization are not readily accessible. It is the fundamental task to find out possible molecular pathways from mechanical and statistical–mechanical points of view.

In the presence of nanofillers who are of the similar dimensions as the polymer chain, one more variable is introduced into the polymer when investigating the kinetics of the crystallization process on molecular level. The crystal growth rate in nanocomposites was investigated by Nitta and col. [21].

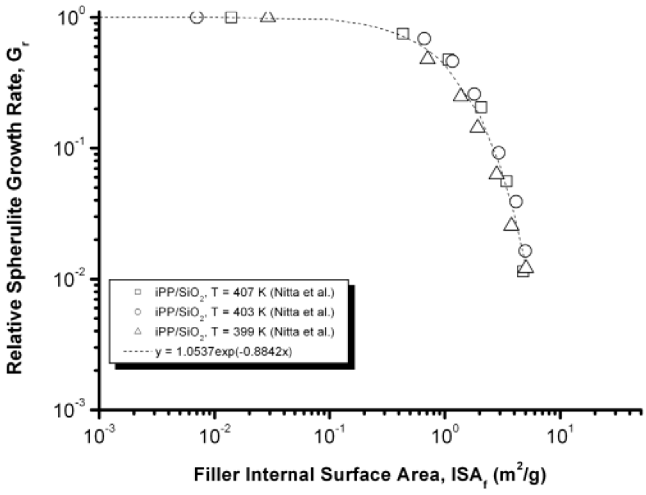

Figure 2: Experimentally measured dependence of spherulite growth rate on internal surface area for iPP-SiO_2 nanocomposite presented by Nitta et al. [21].

For polypropylene filled with nano-silica, it has been shown that the crystal growth rate is reduced with the increasing amount of the filler (Figure 2). The observed behavior was subscribed to the geometrical constraints. Similar trends were observed by Waddon and Petrovic [22] for polyethylene oxide filled with colloidal silica. The focus is given at the behavior at the different crystallization temperatures and slowing down of the crystal growth with the increasing filler content is interpreted in terms of reduced molecular mobility. However, no direct evidence of this interpretation was given. Recently, the approach to view the crystallization behavior in nanocomposites from the point of the dynamic fragility concept has been presented [23]. It has been shown previously that the chain mobility can be considerably reduced in the presence of nano-sized inclusions near and above the matrix glass transition temperature, T_g [24]. Hence, it could be assumed that the presence of weakly interacting silica nanoparticles could result in an increase of the activation energy of chain diffusion, Q_D^*, in the melt resulting in a considerable change in crystallization kinetics, similarly to the trends observed by Nitta for polypropylene.

MATERIALS AND METHODS

Fumed silica (Sigma Aldrich, USA) with specific surface area of 390 m^2/g and mean particle diameter d = 8 nm was used as the nano-filler. This type of silica, who has a spherical shape, has been chosen to eliminate the effect of the filler shape.

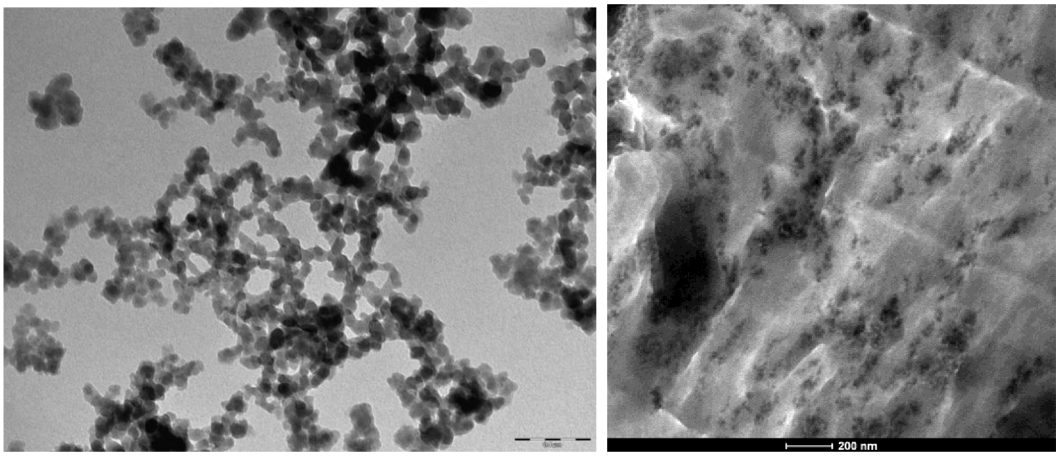

Figure 3: Transmission electron micrograph of the used silica fillers. The tendency of the fumed silica to aggregate is shown. On the right is TEM micrograph of HDPE containing 8 volume % of silica nano-filler. The areas with different filler contents are shown. The various scales are shown with the impact on the various scales.

Commercial high density polyethylene, HDPE, and laboratory synthesized model polyethylene with narrow molecular weight distribution were used as matrices. Homopolymer Liten MB 71 (Chemopetrol, CZ, M_w = 86 000 g/mol (determined by high temperature gel permeation chromatography), M_w/M_n = 5.79) was used as a matrix. Nanocomposites were prepared by adding silica into the xylene solution of HDPE at 130°C under ultrasonic vibrations, intensive mixing and drying at 70°C for 10 hours. Dried nanocomposite powder was compression molded at 170°C using a press (TP 400, Fontijne) into 1 mm thick sheets. The neat PE, used as a reference material, went through the same preparation procedure as the nanocomposites.

Sample	Filler volume content (%)	Specific internal surface of fillers in nanocomposite = filler-matrix contact area (m^2/g of composite)	Specific internal surface of fillers in nanocomposite = filler-matrix contact area (m^2/cm^3 of composite)
Neat HDPE	0	0	0
HDPE 2	2	16	14.1
HDPE 4	4	32	29.1
HDPE 8	8	64	61.8

Table 1: Table of HDPE samples with emphasis on relation of volume filling and the specific internal surface of fillers in nanocomposite.

Model narrow MWD polyethylenes [25] were prepared using phenoxy-imine complex catalyst bis[N-(3-*tert*-butylsalicylidene)-2,3,4,5,6pentafluoroanilinato] titanium(IV)dichloride in combination with methylalumoxane (MAO) as a co-catalyst.

Average molecular weight (M_n and M_w) and polydispersity index (M_w/M_n) of the synthetized model polyethylenes were determined by high temperature gel-permeation chromatograph (Polymer Laboratories) at 140 °C in decalin using polystyrene standards. Melting temperature (T_m) was determined by DSC upon heating sample to 160 °C at heating rate of 10 °C/min. The polyethylene was dissolved in xylene at 90°C, stabilized with Irganox 1076 [26] and the various contents of silica were added (0,2,4,8 volume percent). The volume content was kept so low to be able to capture the onset of the investigated crystal growth change with the present of the filler. Consequently, the samples were placed in the ultra sound bath for 15 minutes and then casted on a hot microscope slide and heated for 15 minutes at 170°C.

The spherulite growth rates were investigated using optical microscope (BX50, Olympus) and hot-stage (LTS 350, Linkam) under isothermal conditions at standard pressure

Prepared films of thickness ranging from 5 to 10 μm were used for crystallization kinetics measurements, thin slices cut out from the pressed sheets were placed between two glass slides. Before each measurement of the spherulite radii, the specimen was melted at 170°C. After 5 min at 170°C, the specimen was cooled down below the melting temperature as fast as the hot-stage allowed. The spherulite growth rate was measured isothermally at temperatures 125°C, 126°C, 127°C and 128°C, respectively. These temperatures were chosen to be in the span of crystallization regime II for polyethylene [13]. The samples for the hot stage were prepared using either solution of melting method. The thickness was determined via confocal laser scanning microscopy (CLSM) as the thickness for the spherulite to have a space to fully develop in 3D. To verify the effect of the nucleation of fumed nanosilica in the matrix, the method suggested by Dobreva has been employed [27]. The samples were heated in a differential scanning calorimeter (Pyris 1, Perkin Elmer) up to 170°C at a rate of heating 10°C/min. After 2 minutes at 170°C, cooling down to the room temperature was carried out at rates of cooling 2, 5, 10, 20 and 40°C/min, respectively. Crystallization temperatures were obtained from the DSC peak maxima. SEM and TEM are utilized to study aggregation of the particles.

Within this thesis molecular dynamics (MD) and Monte Carlo (MC) methods are employed. Molecular dynamics solves the Newton´s equation of motion with time, the temperature or pressure being kept by coupling to thermostat or barostat, respectively. Monte Carlo method, as suggested by its name, operates on the basics of chance events. The motion is random and mimics the Boltzmann distribution function [28]. A united atom interaction potential was used, in which polymer chains are represented by CH_2 and CH_3 beads that interact via bonding and non-bonding interactions. The importance of using the realistic potential has been shown as crucial for the balance between orienting and crystal packing

process. United atom force field for polyethylene melts derived by Paul and coworkers (PYS) [29] has been employed in this thesis. The non-bonded potential for atoms separated by more than three bonds follows the Lennard-Jones (LJ) relation [29]:

$$E_{NONBOND} = 4\varepsilon\left[(\sigma / r)^{12} - (\sigma / r)^{6}\right], \quad (1)$$

where ε = 0.0504 kJ/mol and equilibrium reference distance σ = 4.01Å with a given cut off distance of 12Å. LJ potential is particularly important in the bulk systems. By variation in LJ particle-matrix interactions the different type of interactions has been set up (Table 2).

	Weakly interacting	Strongly interacting	None	Repulsive
Sigma	4.01Å	4.01Å	4.01Å	4.01Å
Epsilon	0.0504 kJ/mol	0.504 kJ/mol	0 kJ/mol	0.0504 kJ/mol From 0.2 Å : 0 kJ/mol

Table 2: Lennard-Jones potential parameters

The system of 100 chains, each one containing 100 units, was generated by Monte Carlo method respecting the potential field presented. The script was written in C/C++ programming language. The bond lengths and bond angles were kept constant and the torsional angles were distributed according to the Boltzmann distribution at the given temperature. The bulk sample was generated at the reduced density 0.3g/cm^3, because at higher densities the probability to find the acceptable free The Nose-Hoover temperature coupling was utilized with time constant t = 0.1ps. As for the single chain system, velocities at the temperature 500K were generated by the Maxwell distribution and first 5ns of the simulation were taken as equilibration of the system.

The nanoparticles consisted of 46 Lennard-Jones particles bound to form icosahedral shape (Figure 4). It was inserted into the nanocomposite prior the generation of the melt .The diameter of the particle was 2nm. Consequently, the sample was allowed to equilibrate at 500K for 1ns.

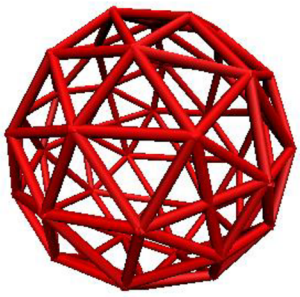

Figure 4: The nanoparticle representation. The Lennard-Jones particles are in the tips of the icosahedral object. The interaction radius of each particle is dependent on the filler-matrix interaction type (Table 2).

According to Yamamoto [30], the crystal surface was defined as the aligned chains in the *xy* plane with the interlayer spacing of 3.78 nm which corresponds to the crystal facet (100). The starting simulation box was 27x80x70A. As we are investigating the crystal growth itself not the nuclei formation or initiation period, this definition of the crystal surface has proven to be in line with the polymer physics.

The standard measure of order used in polymer systems is the global bond orientational parameter at time *t*

$$S(t) = \frac{3\left\langle \left[v_i(t) \bullet v_j(t) \right] \right\rangle}{2} - \frac{1}{2} \quad , \qquad (2)$$

where $v_i(t)$ is the orientation vector of atom *i* at time *t*, defined by the chord from atom *i*-1 to atom *i*+1, and the average is taken over all pairs *i* and *j*. However, in order to calculate the spatial distribution of order within the simulation box a local orientation order must be defined. The method implemented by Waheed [31] based on the convolutions of the local chain orientation vectors with spatial box functions is utilized. .

For nanocomposites, the samples were equilibrated for 1ns at the temperature of 500K. The simulation was conducted in the NVT ensemble (constant number of particles (N), volume (V) and temperature (T)) at the temperature of 400K. The molecular simulation package Gromacs 4.0.5 [32] has been used to perform the computer simulation and Visual Molecular Dynamics [33] was utilized for visualization. The computational cost was 25.797 Mnbf/s, simulations were conducted to 100ns. The scheme of the model arrangements is shown in Figure 5.

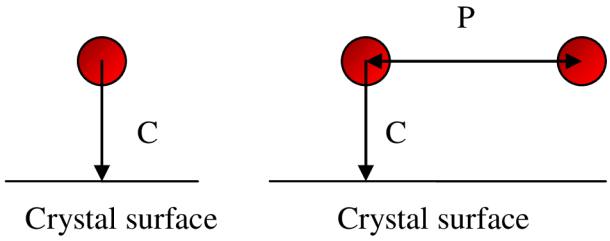

Figure 5: The experiment arrangement for single particle and two particles. The arrows sign the distance from the crystal surface and the inter-particle distance, respectively. C stands for the distance from the crystal surface and P for the distance of particle centers, respectively.

RESULTS

The nucleation effect and aggregation of the fillers

Although this work is primarily focused on the subsequent spherulite growth, it is important to investigate the possible heterogeneous nucleation activity and the aggregation effects of the fillers that could affect the crystallization kinetics and its interpretations, significantly.

Utilizing the SEM micrographs and the method of Dobreva [27] suggests that the silica nano-filler used in our experiments did not exhibit any significant nucleation activity in HDPE matrix under the experimental conditions used.

Nanometer sized silica particles tend to form more complicated structures, depending on the matrix – filler interaction type and solidification process [34]. In addition to forming particle strings upon synthesis, the fumed silica has a strong tendency to aggregate in polymer matrix similarly to colloids. This results in formation of island like structure of resin rich and particle rich areas (Figure 3). The TEM micrograph on the right has been taken for the HDPE filled with 8 volume % of fumed silica. Within this thesis, surface treatment of the silica nanoparticles would introduce another entity into the matrix-filler interface, changing the dynamics in the investigated area. Thus, to overcome the aggregation issue, the ensemble of the representative samples of the nanocomposite was chosen and the results were averaged.

The Spherulite Growth Rate

The spherulite growth rate was investigated utilizing polarized optical light microscopy equipped with a hot stage. The thickness of the sample for the experiments was 5-10μm to allow the full development of the three dimensional structure. The growth rates were measured isothermally with the medium level undercooling corresponding to crystallization regime II where the effect of particles on the chain reptation is expected to be the most pronounced. For polyethylene, this range corresponds to crystallization temperatures in the range of 120-129 °C [13]. The results of 10 measurements were averaged to determine the average growth rate, G.

The micrographs of the growing spherulites are shown in the Figure 6. They were taken for the neat polyethylene at the temperature 127°C, the interval between the shots was 5 minutes and the right micrograph exhibits the final stage when the crystal growth observable by the polarized microscopy is finished. The black areas correspond to the amorphous parts while the light ones correspond to the crystalline phase. The light objects are crystals of HDPE. In time, the spherulitic structure starts to emerge and grows until the crystals impinge each other at the boundaries.

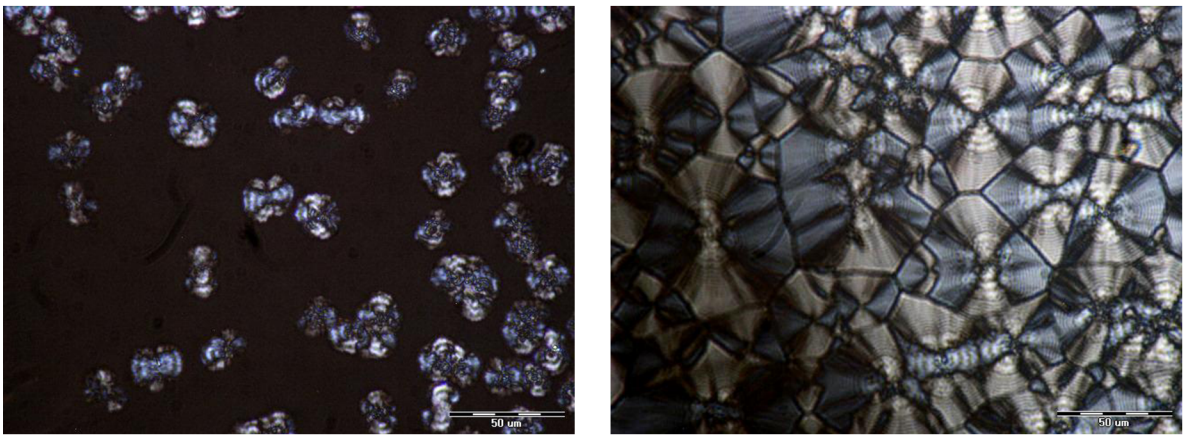

Figure 6: The micrographs of the growing spherulites in the neat HDPE at 127°C. The micrograph on the right corresponds to the observable final structure.

The crystal growth rate was determined from the polarized optical light micrographs taken automatically at suitable time intervals, as an increase of spherulite radius in time. As expected, the growth of the spherulites was linear in time. Then, the final growth rate G_{II} was given by the slope of time dependence of spherulite radii. It can also be seen that the slope of the linear R vs. t dependence decreased with the increasing filler content (Figure 7).

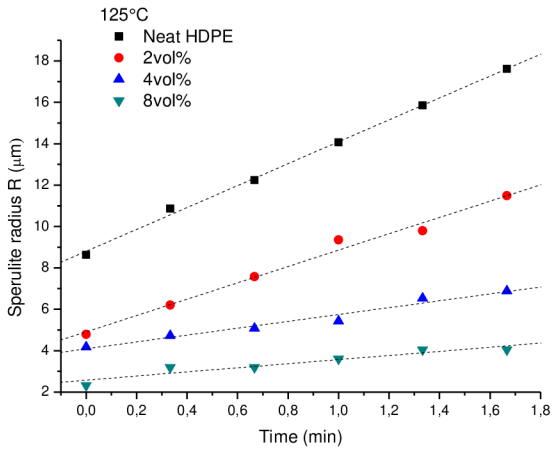

Figure 7: The example of the linear time dependence of spherulite radius R at the temperature 125°C for HDPE/silica nanocomposite with filler content 0, 2, 4 and 8 volume % (specific internal surface 0, 16, 32 and 64 m^2/g of the filler in nanocomposite.

With the increasing area of the matrix-filler interface, for the sample with 8 volume % of silica, the growth rate was reduced to approximately 20%of its value for neat PE. This trend has been observed for the whole range of investigated temperatures in the crystallization regime II. In agreement with the crystallization thermodynamics, the crystallization rates were faster for higher undercooling (Fig. 8 on the left, melting temperature T_m = 135°C, temperature of maximum crystallization velocity T_{vmax} = 46°C [3]). However, the trends of the crystal growth dependence on the content of the fillers are very similar in the whole

temperature regime (Figure 8 on the right). The crystal growth was investigated, thus, the nucleation time was not important in this experiments.

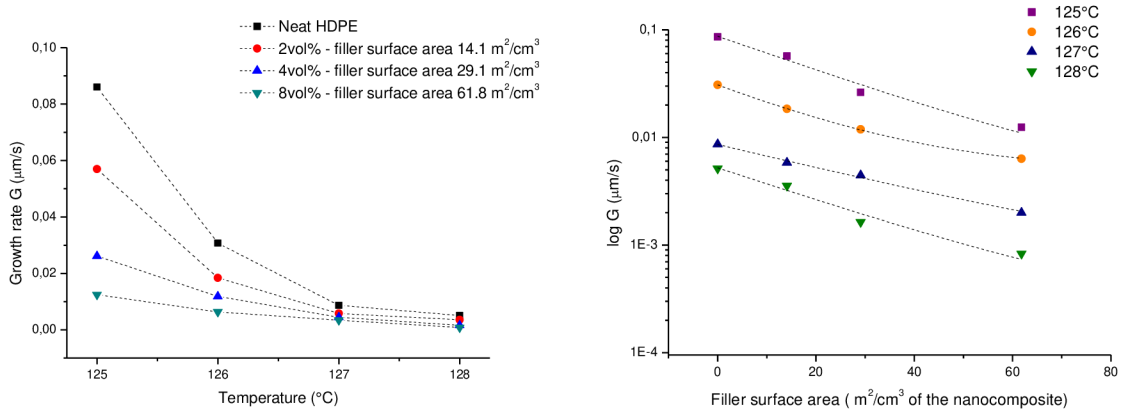

Figure 8: On the left, the growth rates dependence on the undercooling for the samples of neat polyethylene and nanocomposite. The diffusion changes are more pronounced at lower temperatures, there are only weak interaction present between the matrix and the filler. On the right, trends of spherulite growth rate G in dependence on the matrix-filler interface area.

Comparison of experimental results with the L-H theory predictions

To be able to separate various contributions that cause the observed reduction of the crystal growth rate, experimentally measured growth rate data were compared with the predictions based on the Lauritzen Hoffman secondary surface nucleation theory with the incorporated terms for activation energy of the reptation motion [12].

The growth rate observed via polarized light optical microscopy corresponds to the G_{II} in this theory. The activation energy Q^*_D has been taken as a variable parameter to correlate the calculated trends with experimental data. For the neat HDPE, the curve has been fitted to the experimental data and corresponding activation energy value was found to be 24 kJ.mol^{-1} which is in excellent agreement with the activation energy for the reptation motion for PE published in the literature which is in the range from 20 to 25 kJ/mol [37,38]. The comparison of L-H prediction for neat HDPE and the experimentally measured G_{II} for the neat and silica filled HDPE is shown in Figure 9.

Moreover, it was found that with increasing filler-matrix interface area, the Q^*_D calculated from the L-H theory followed the observed trends and increased significantly up to the 108kJ.mol^{-1} for 8vol % of silica. Thus, it can be suggested that in the presence of the weakly interacting surface, the reptation motion was retarded and extend of immobilization increased with increasing filler-matrix interface area. Assuming interphase layer thickness equal to approximately $1R_g$ (3.74 nm for the HDPE) the diffusion activation energy from the L-H theory can be estimated as $Q_D^{interphase} = 2Q_D^{neat}$. This trend was shown valid over the entire undercooling regime II.

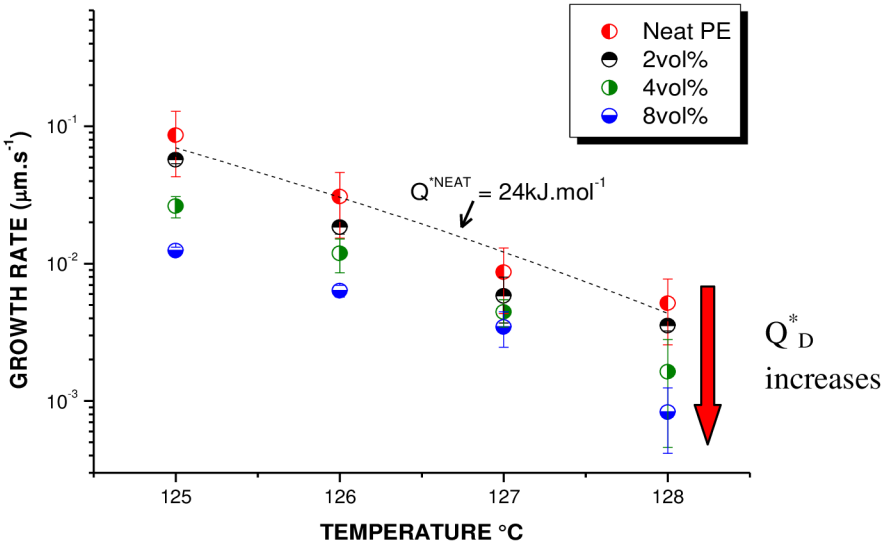

Figure 9: Spherulite growth rate of neat and nano-filled HDPE in dependence on temperature.

Molecular weight scaling of the crystals growth rates

From reptation theory, the diffusion coefficient, D, dependence on molecular weight M is predicted as $D \sim M^{-2}$ [40]. Including two additional effects, constraint release (CR) that happens when a spatially confined chain moves out of the way of a given chain and, thus, opens some space for lateral motion and contour length fluctuations (CLF), when the chain contracts in its tube and after subsequent expansion it loses memory of the initial tube and the D scales as $D \sim M^{-2.30 \pm 0.1}$ up to $M \cong 10^3$ instead of by reptation predicted $D \sim M^{-2}$ [41]. Since the crystal growth rate is measured in relatively thin films in our experiments, the diffusion could be spatially limited to the two dimensions. The geometrical dimensions could also be changed with the chains confinement due to the particle presence.

In this experimental study, the well defined polyethylenes with polydispersity index close to 1 were utilized. For the molecular dynamics considerations, the number molecular weight average, $\overline{M_n}$, was used. The molecular weight was chosen to vary from 64800 to 146800.

Again, the growth rate of the crystal formation has been determined as a slope of crystal radius time dependences. Similarly to the commercial HDPE, all R vs. t dependences were linear. In agreement with the observations in commercial HDPE, the slopes are lower with the increased matrix-filler interface area. As expected, crystallization temperature exhibited much more pronounced effect for low molecular weight PE. It is important finding that growth rate dependencies on temperature in the crystallization regime II are the similar for the neat system and both nanocomposites that suggests that in the presence of the fillers no additional change in the crystallization mechanism can be expected.

The absolute value of G_{II} decreased with increasing amount of silica and increasing molecular weight of PE, however, the scaling exponent remained constant within the experimental error (Table 3). The scaling of crystal growth rate with M_n obeys the reptation plus CLF prediction, $D \sim M^{-2.30 \pm 0.1}$, for both neat and filled PE. This supports the hypothesis that chain reptation remains the main means of mass diffusion to the growing crystal face. With the observed molecular weight scaling of crystals growth rates it is possible to suggest, that the crystal growth rate reduction observable with addition of silica nanoparticles to the PE is of the reptation type and can be contributed to the immobilization effect of the presence of a large internal surface area.

Moreover, the dependence is of the same strength not as it would be expected with changing fragility. Dynamic fragility of the glass forming liquids and fragility index, respectively, reflect the rate of change of the dynamic properties with temperature. From the point of molecular weight, lower molecular weight materials have a higher mobility and thus shorter relaxation times. Thus, the lower fragility is connected with the weaker molecular weight scaling.

Molecular weight dependence	125°C	126°C	127°C
Neat PE	-2.348	-2.348	-2.253
2 vol % filler	*-2.301*	*-1.967*	*-2.034*
4 volume % filler	*-2.267*	*-2.161*	*-2.165*

Table 3: Scaling of the crystal growth rate with molecular weight. The exponential coefficients are listed here.

The increased entanglement density [42] can be one of the mechanisms causing the retardation of chain reptation with adding the nanoparticles into the polymer matrix. In the reptation theory [40], entanglement is viewed as a topological constraint to the chain dynamics. The reduction of the crystal growth rate in the presence of fillers with large specific surface area then can be a result of apparent increase of the effective number of entanglements per chain reducing the reptation tube diameter. Considering the average entanglement length of polyethylene chain in neat PE equal to 35 monomeric units [43], it is possible to ascribe the decreased crystal growth rate to the increased number of effective entanglements (Figure 10).

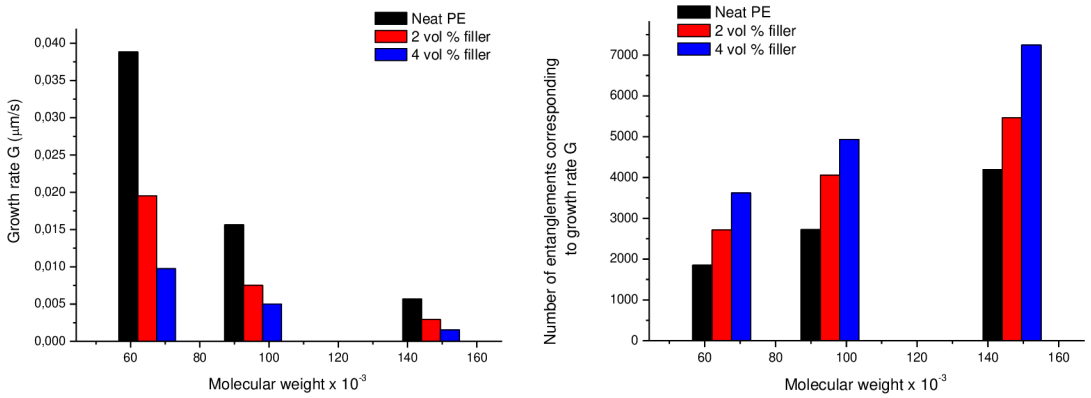

Figure 10: The crystal growth rates at 125°C. The rate decreases with the increasing of the filler content and with increasing molecular weight of the matrix. On the right, the effective number of entanglements calculated from the crystal growth rates at 125°C.

For PE containing 2 volume % of silica, the number of effective entanglements was increased by factor 1.41 and for PE containing 4vol% of silica by factor of 1.83. The same trend is valid for all temperatures investigated (Figure 11). The trends still follow the reptation expected scaling of the dependence on molecular weight. Based on these results, it can be assumed that the reduction of the crystal growth rate can be interpreted as a result of increased number of effective entanglements per a polymer chain, in agreement with the theory of the chains immobilization at the particle surface.

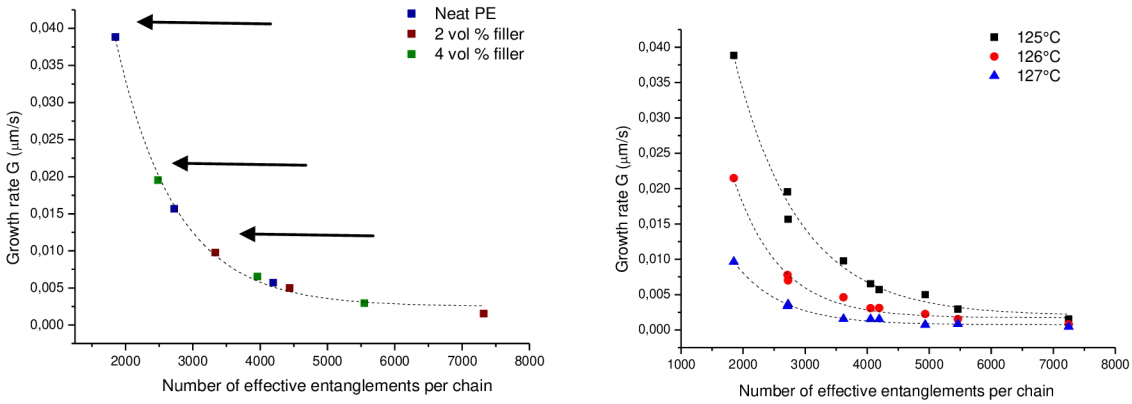

Figure 11: Dependence of the growth rates based on the effective number of entanglements calculated from the crystal growth rates at 125°C. Shift factors are 1 for neat system, 1.41 for nanocomposite containing 2vol% of silica filler and 1.83 for nanocomposite with 4vol% of fillers, respectively. The arrows show the matrices with in reality the same molecular weight. On the right, plot of the growth rates based on the effective number of entanglements calculated from the crystal growth rates at all temperatures, applying the shift factors from the figure.

Molecular dynamics simulations

The L-H theory provides sound support for the hypothesis that the crystal growth rate reduction is mainly due to the immobilization of the chains at the particle surface and thus, due to the retarded diffusion of chains to the growth front. However, due to its semi-empirical nature, the need for a computer simulation arose. As the observed phenomena take place on the molecular level, the molecular dynamics and Monte Carlo simulations were employed to give further insight into the phenomena investigated. The systems were created step by step to verify the physical basis of the given stage before moving to the higher stage. It is necessary to bear in mind that computer simulation still posses many assumptions and limitations (e.g. much shorter chains, short times, etc.) and, thus, they are used to show the trends rather than to calculate actual values of parameters investigated.

Prior inserting the nanoparticle into the system the physical properties of chain and bulk and the crystallization of the neat polymer was performed and compared with experimentally available data.

Single chain system was created to the test of the physical properties and correctness of the used parameters and methods. The chains of 1000, 2000, 3000 and 5000 units were used as samples. Simulation temperatures were 500K, 400K, 300K, 200K and 100K. The Nose-Hoover temperature coupling was utilized with time constant t = 0.1ps. Velocities at given temperature were generated by the Maxwell distribution. First 5ns of the simulation were taken as equilibration of the system. Neat PE has been modeled as an ensemble of 100 chains each consisting of 100 segments. The characteristic ratio was found to be 5.7 which is in good agreement with Boyd and Philips giving value of 6 for the chain length of 100 units [38]. The ratio of the chain radius of gyration and end-to-end distance was higher than 6, thus, the systems due to the short chain lengths should not be treated as a Gaussian chain. The R_G calculated based on the theoretical model by Flory for the chain of 100 was 3.74 nm.

The crystal development was observed in three layers utilizing the order parameter development, the example of the emerging order is shown in the Figure 12. During the simulation, the additional crystalline order starts to develop on the primarily crystal surface. The first peak on the left side of the graph stands for the primarily crystal surface, the second and further are signifying the crystalline structure ordering. The peaks on the right emerge due to the periodic boundary condition in the simulation settings.

The time dependence of the observed order parameters depicted in Figure 12 is similar to that simulated by Waheed et al. [31] utilizing the Steel type potential field as a crystalline surface. The green line corresponds to the order of the primarily inserted crystalline surface of polyethylene, the black, red and blue show the order development in time for the newly created crystalline layers. The growth rate of the composite was determined for each sample by the completion of the ordering in the crystallization plane averaged over the first two crystalline layers emerging during the simulation at the primary surface of polyethylene crystal.

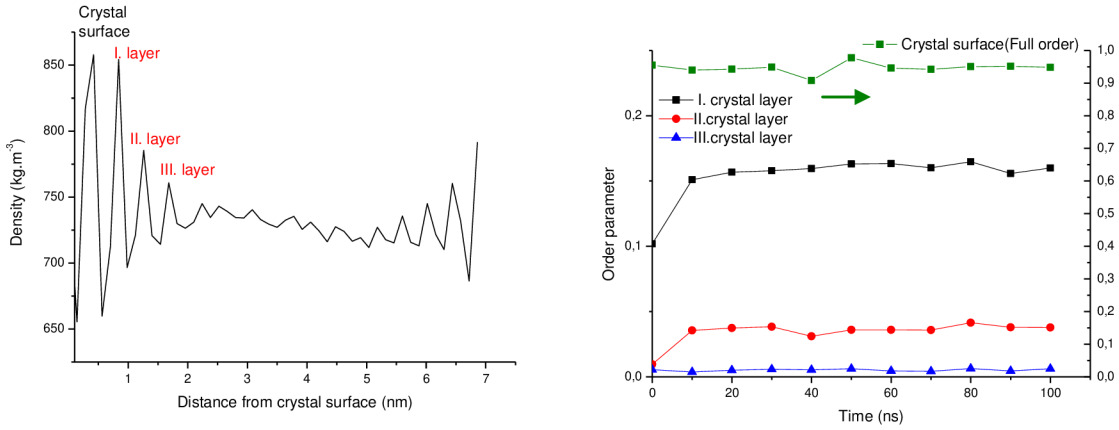

Figure 12: Example of the density profiles utilized to detect the positions of the growing layers. The minima between the peaks were used to set the layer boundaries for each measurement on the left and example of the order parameter used to calculate the growth rate or the crystalline order formation, respectively. The points are the times when the order was analyzed. The simulation of each system was up to 100ns. For each simulation of this type was analyzed.

The simulated crystal growth rate for the neat polymer was found to be 4.10^{-4} nm.ns^{-1}. This value fits the theoretical predictions of van Krevelen and Strobl and is in agreement with the simulations data of Waheed [3, 31, 36]. The maximal experimentally obtained value for the crystal growth rate was of the order of 1.10^{-5} nm.ns$^{-1.}$ The difference between experimental and theoretical value could be ascribed to the higher molecular weight of the experimentally measured samples and, thus, higher entanglement density. Also, simulation techniques operate on molecular scale and experimental techniques probe the problem starting on a macroscale, thus, the direct comparison can face a certain difficulties.

The crystallization in the presence of a nano-filler

In Figure 13, the snapshots of the polymer chains order being created near the crystal surface are shown. The dashed arrow shows the original inserted crystal surface at which the crystallization order occurs. The full ones are showing the simulated development of the structure with time. Red icosahedral in the middle of the figure is the nanoparticle. It is expected that the nano-filler should significantly change the development of the crystalline layers in the simulated system. The matrix-filler mutual interactions were altered in order to separate the various contributions to the crystal growth. The diameter of the particle was 2nm.

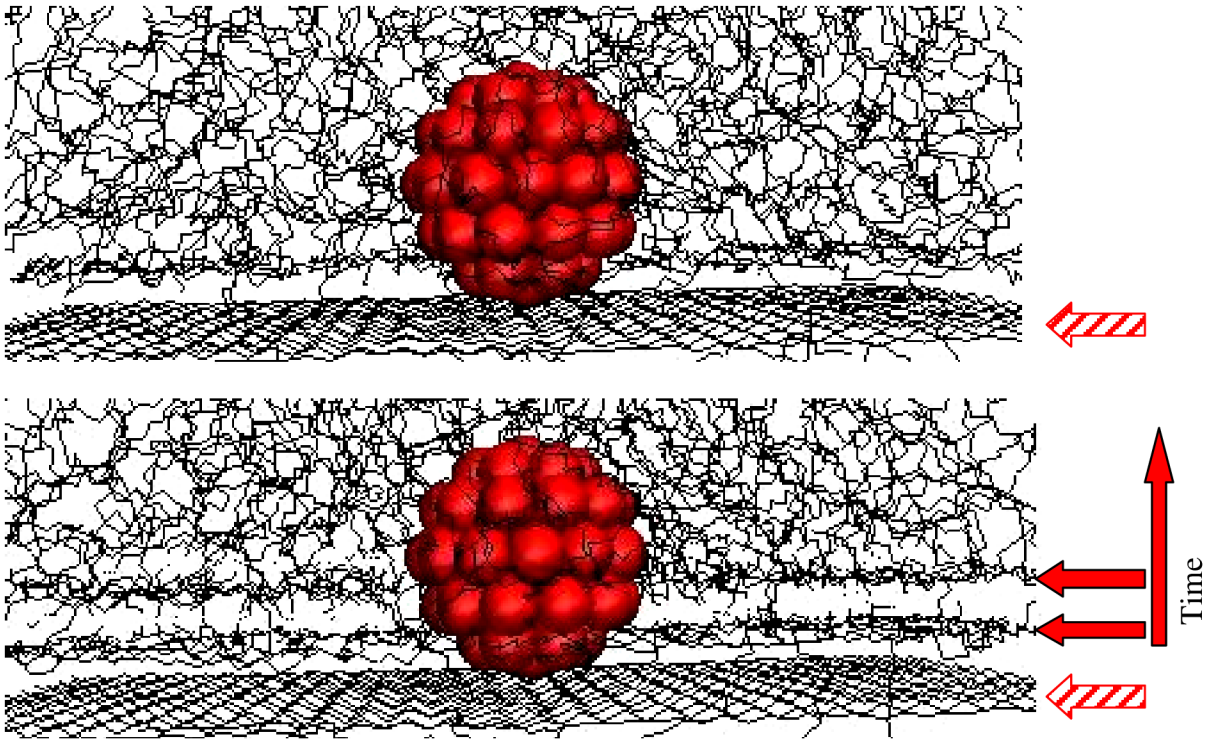

Figure 13: The snapshots of the crystal growth at the simulation start and after 30ns.The textured arrows stand for the primary crystal surface while the red full arrows signify formation of the new lamellae in time of the computer simulation.

In Figure 14, one can compare that order development rates in the case of strongly or weakly interacting particle is lower than in neat polymer. For the repulsive or non interacting particle, no significant perturbation of the order development is observable, when the crystal surface is in a distance from the particle (on the left 2.4 nm) where the entanglements can transfer the immobilization effect to the distance more far from the actual immobilization site at the particle surface. These trends are reproduced also when moving the particle closer to the crystalline surface. When the primary crystal surface is close to a particle, the geometrical constraints are becoming more pronounced. The emphasis has been given to the comparison of the crystal growth rates with different type of interactions. As shown in Figure 13, the experimentally observed retardation is dominant only in attractive system and increased with the attractive interaction strength. The geometrical effects are supposed to happen due the constraints imposed on the chains in the inter-particle spaces and distance of the particle from the crystallizing surface. No increase in the growth rate for repulsive particle-matrix interaction in comparison with the final growth rate in polymer suggested that the dynamic fragility concept cannot be used. For the attractive filler-matrix potential, the chain packing at the surface is more perturbed in comparison with a neat melt. This can result in a higher structural frustration in a nanocomposite material.

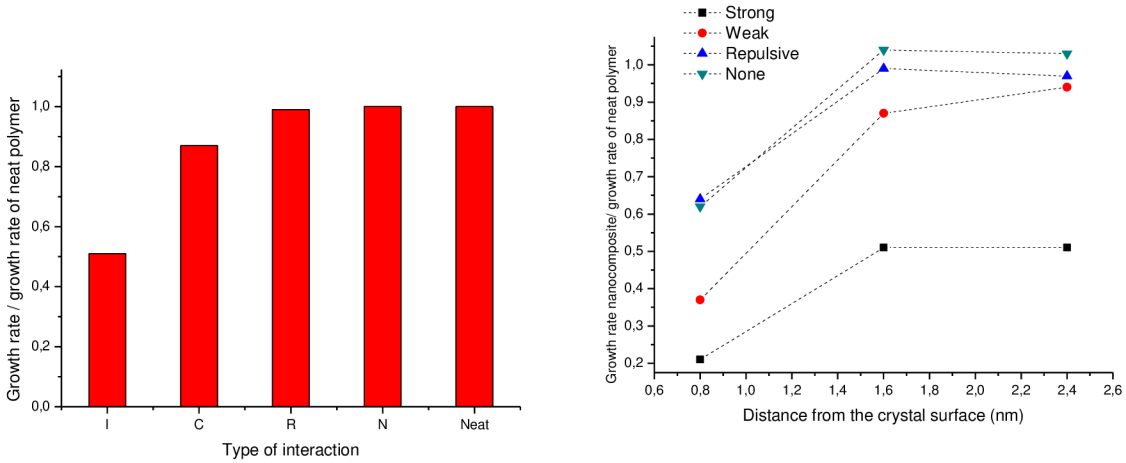

Figure 14: The ordered structure development for the simulated HDPE nanocomposite with silica content 1.81vol %, comparison of the various interaction types. The values are taken relatively to the neat system. On the right, the relative crystal growth rate for the various particle-chain interactions in dependence on the particle distance from the crystal surface. Silica content 1.81vol %.

Even more insight into the phenomenon was given by simulating the effect of two particles on G_{II}. In the comparison with the results for one particle, it can clearly be seen that adding second particle makes the simulation more realistic resulting in further decrease in the crystalline order development rate depending on the particles-matrix interaction, mutual position of the particles and the distance from the crystal surface.

For strong attraction, the crystal growth is significantly retarded at all distances from the surface investigated. This, in lesser extent, was valid also for the weakly interacting systems (Figure 15). In contrast, the repulsive and non-interacting systems tend to slow down the order formation only in the very close vicinity of the crystal surface. Very importantly, for non-attractive systems, no significant difference was obtained between the tendencies of system with one and two particles for the same distance from the crystal surface (Figure 16).

It is possible to see that the chain dynamics retardation in the vicinity of the particle surface is controlled by the chain-particle interaction strength. The restrictions observable also for the non-interacting and repulsive types never reach such a scale as in the case of interacting filler.

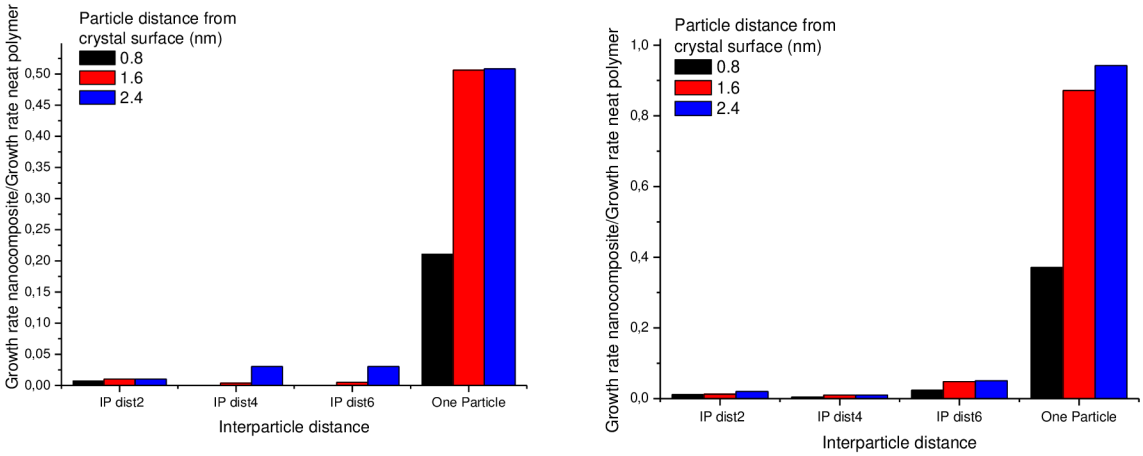

Figure 15: Comparison of the crystal growth rates single particle- double particle in dependence on the particles distance from crystal surface. The strong interactions are on the left and weak mutual interaction on the right.

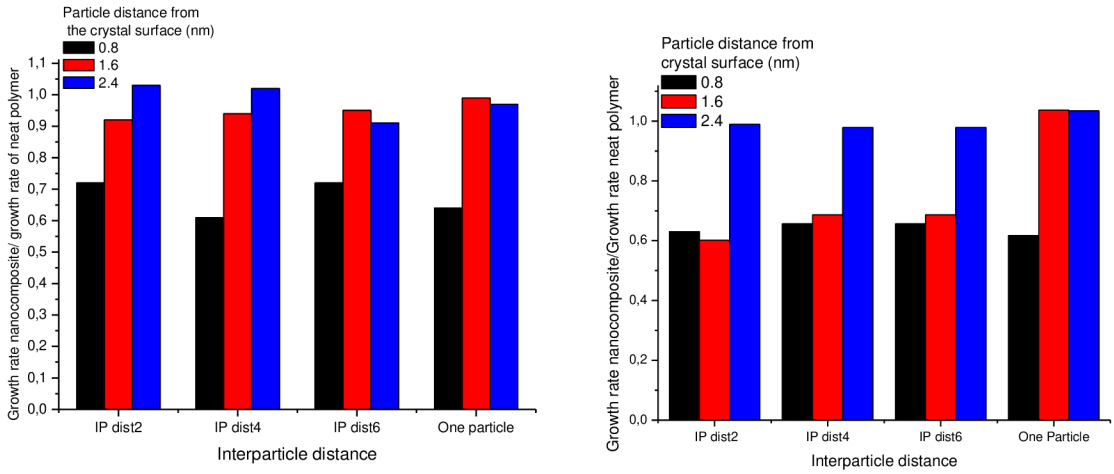

Figure 16: Comparison of the crystal growth rates single particle- double particle in dependence on the particles distance from crystal surface. The repulsive interactions are on the left and none mutual interaction on the right.

What is important here is that with moving of the particle closer to the crystal surface the growth rate decreases. This trend is true for all the particle centers distances. It can be interpreted as the larger amount of the immobilized chain units present in both the crystallizing surface and the particle interfacial area. As an example, the dependency for the particles center distance 2nm is shown (Figure 17).

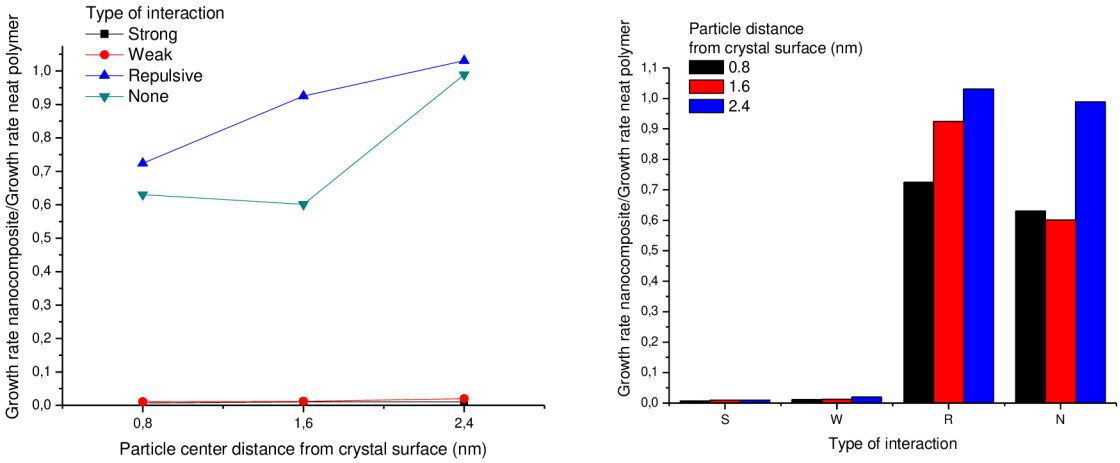

Figure 17: The order development rates in dependence on the distance of the particles from crystal surface and for various interaction types (left). The distance of particle centers is constant (2nm). I stands for strong interaction, C-weak interaction, R-repulsive, N-non-interactive system, respectively.

When moving particles closer to each other while keeping their distance from the crystal surface constant, the vertical confinement enhanced the possibilities to create a simple particle-polymer network via bridges or loops. The following figure (Figure 18) shows, that with the decreasing inter-particle distance, the crystal growth rate remains unaffected within the experimental error. These data suggest that the vertical confinement of the chains is not playing an important role in the chains immobilization. It implies, the bridging effects had no significant effect on the crystal growth rate in the model PE/silica nanocomposites.

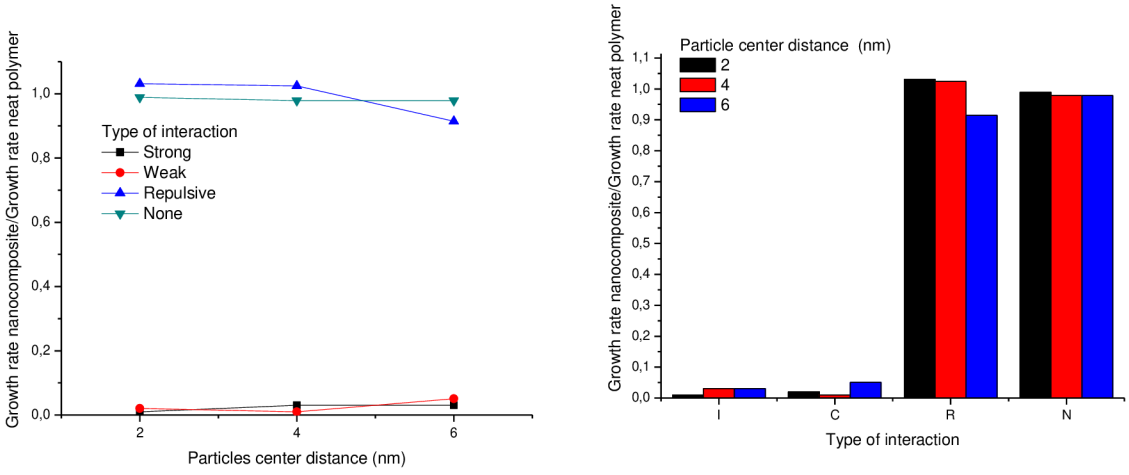

Figure 18: The order development rates in dependence on the distance of the particles centers and for various interaction types (left). The distance from the crystal surface is constant (2.4nm. I stand for strong interaction, C-weak interaction, R-repulsive, N-non-interactive.

CONCLUSIONS

Within frame of this PhD work the isothermal crystallization of neat HDPE has been investigated using the polarized light optical microscope and hot stage. The results clearly showed that the rate of spherulite growth was substantially decreased by the addition of silica nanoparticles. In order to explain the observed crystallization behavior interpretation based on the assumption that the segmental diffusion is considerably reduced in presence of nanoparticles has been suggested. To verify the proposed hypothesis, the experimental data were correlated with Lauritzen- Hoffman secondary surface nucleation theory. The role of the fillers nucleation and aggregation was included. The nanocomposite nucleates homogeneously and uniformly within the sample. Further on, the molecular dynamics simulations on molecular level were performed.

The following evidence supporting the immobilization theory has been observed: The correlation of the experimentally measured decrease in crystal growth rates with the Lauritzen-Hoffman secondary surface nucleation theory clearly showed the increase of the activation energy of the reptation motion with the increased internal surface area of the filler. The molecular weight scaling was following the reptation prediction with the contour length fluctuation included. The results clearly showed that the reduction of the crystal growth rates can be interpreted via immobilization theory as the increased number of effective entanglements. From the molecular dynamics simulation as the primary mechanism affecting the morphology development was identified the mutual particle-matrix interaction type and thus the immobilization of the chains at the filler surfaces. Based on these results, the crystal growth and thus the morphology formation in the filled systems should be up to the certain threshold tailored by altering the mutual interactions.

The significance of the obtained results is twofold. First, knowledge of the fundamental processes affecting the chain dynamics in the presence of particles with size of the order of the radius of gyration of the chains was gained. Second, quantification of the relationships between structural variables, crystallization kinetics, crystalline structure and deformation response in polyolefin nanocomposites can provide a base for developing new advanced high volume polymer materials for a wide range of applications. The computer model will help to understand and predict properties of semicrystalline nanocomposites by allowing optimizing of the composition and processing conditions. Results of this research can also contribute significantly to the basic understanding of the effects of chain immobilization on various aspects of behavior of nanostructured polymeric systems in both molten and solid state.

REFERENCES

[1] B. Wunderlich, Macromolecular physics vols. 1–3, Academic, New York (1976).

[2] Woodward, A.E., *Atlas of polymer morphology*. **1988**, Munich, Hanser publishers, 25,47.

[3] van Krevelen, D.W., *Properties of Polymers*, Elsevier, Amsterdam, **1997**.

[4] Strobl G., *The physics of polymers*, Springer, 2006.

[5] H. Tadokoro, Structure of crystalline polymers, John Wiley and Sons (1979).

[6] E.A. Colboun and J. Kendrick, previous termComputernext term simulation of polymers, Longman Scientific & Technical (1994).

[7] G. Rutledge In: M. Kotelyanskii and D.N. Theodorou, Editors, Simulation methods for polymers, Marcel Dekker, New York (2004).

[8] Interphases and mesophases in polymer crystallization. In: G. Allegra, Editor, Adv. Polym. Sci. vols. 180, 181, 191, Springer, Berlin (2005).

[9] L. Mandelkern, Crystallization of polymers vols. 1–2, Cambridge University Press, Edinburgh (2002).

[10] D.C. Bassett, Principles of polymer morphology, Cambridge University Press (1981).

[11] Yamamoto T., Orimi N., Urakami N., Sawada K., *Molecular dynamics modeling of polymer crystallization; from simple polymers to helical ones*, Faraday Discuss., **2005**, 128, 75-86.

[12] J.D. Hoffman and R.L. Miller, Polymer 38 (1997), p. 3151.

[13] K. Armistead and G. Goldbeck-Wood, Adv Polym Sci 100 (1992), p. 219.

[14] Hoffman, J. D.; Lauritzen, J. I. Jr.; J Res Natl Bur Stand - A **1961**, 65, 297.

[15] Hoffman, J. D., Frolen, L.J. Ross, G.S., Lauritzen, J. I. Journal of Research of the National Bureau of Standards Sectiona-Physics and Chemistry **1975**,79(6),671-699.

[16] K. Kaji, K. Nishida, T. Kanaya, G. Matsuba, T. Konishi and M. Imai, Adv Polym Sci 191 (2005), p. 187.

[17] K. Kaji, K. Nishida, T. Kanaya, G. Matsuba, T. Konishi and M. Imai, Adv Polym Sci 191 (2005), p. 187.

[18] G. Reiter and J.U. Sommer, J Chem Phys 112 (2000), p. 4376.

[19] P. Huang, L. Zhu, S.Z.D. Chen, Q. Ge, R.P. Quirk and E. Thomas et al., Macromolecules 34 (2001), p. 6649.

[20] Y. Loo, R.A. Register and A.J. Ryan, Phys Rev Lett 84 (2000), p. 4120

[21] Nitta, K.; Asuka, B.; Liu, M.; Terano; *Polymer* **2006**, 47, 6457.

[22] Waddon, A.J, Petrovic, Z.S.: Polymer Journal, 2002, 34, 876.

[23] Douglas, J., Kumar, S.: discussion within the workshop "Late night show on polymer nanocomposites II, Brno, CR, 2009.

[24] Kalfus, J.; Jancar, J.; *J Polym Sci: Part B: Polym Phys* **2007**, 45, 1380.

[25] Merna, J.: Koordinační polymerace alkenů katalytickými systémy na bázi přechodových kovů. PhD thesis, FCH VUT Brno, 2005.

[26] Sheet: http://www.tri-iso.com/SiteAdmin/Portals/0/12_238_Irganox%201076.pdf

[27] Dobreva A, Gutzov I, J Non-Cryst Solids **1993**; 162:1.

[28] Frenkel, D. and Smit, B. *Understanding molecular simulations from algorithm to applications, 2 edn*, **2002**, Academic press, San Diego.
[29] Paul, W. , Yoon D.Y. ,and Smith, G.D. Journal of Chemical Physics 103 **1995**, p. 1702.
[30] Yamamoto T., Orimi N., Urakami N., Sawada K., *M*, Faraday Discuss., **2005**, 128, 75-86.
[31] Waheed, N., Ko, M.J.m Rutledge, G,C., , Polymer **2005**, 46,8689-8702.
[32] Hess, et al., *J. Chem. Theory Comput.* 4: 435-447, 2008.
[33] The images were made with VMD software support. VMD is developed with NIH support by the Theoretical and Computational Biophysics group at the Beckman Institute, University of Illinois at Urbana-Champaign.
[34] Kumar SK, NanoLett,2008.
[35] Kumar S, *Late Night Show on Nanocomposites II*, Brno, presentation,2009
[36] Strobl G., Prog. Polym. Sci, 31, 2006, 398-442.
[37] Zarzycki J, editor. Glasses and amorphous materials. Materials science and technology, vol 9.
[38] Boyd, R.H, Philips, P.J., , Cambridge University Press.
[39] van Krevelen, D.W., *Crystallinity of polymers and the means to influence the crystallization process*. Chimia **1978**, 32(8),279-294.
[40] de Gennes, P.G., Cornell University press, Ithaca, **1979**, NY.
[41] Ewen B., Richter D., Neutron Spin Echo Investigations on segmental dynamics of polymers in melts, network and solutions. Vol 134, pp 1-130.2005.
[42] Bueche, F., *In reinforcement of elastomers*, Interscience: New York, **1965**.
[43] Kremer, K. and Grest, G.S., , J. Chem. Phys. **1990**, 92(8),5057-5086.

ACKNOWLEDGEMENTS

This work has been supported by Czech ministry of Education, Sports and Youth project MSM 0021630501 and Czech Grant Agency project P205/10/2259.

Author would love to thank for help, support and motivation, when needed, for a useful discussions and hints, personal example in both science and life. Meeting some of them has changed my life in a significant way.

If I may name a few of many my acknowledgements go for, they would definitely be Josef Jancar, Jaroslav Kučera, Lukáš Recman, Jirka Sadílek and Martin Moos.